Thermal-Structural Coupled Analysis of ITER Torus Cryo-Pump Housing*

WANG Songke (王松可), SONG Yuntao (宋云涛), XIE Han (谢韩),
LEI Mingzhun (雷明准)

Institute of Plasma Physics, Chinese Academy of Sciences, Hefei 230031, China

Abstract An ITER torus cryo-pump housing (TCPH), which encloses a torus cryo-pump, is connected to a vacuum vessel (VV) by a set of associated double bellows. There are complicated loads due to two different operating states (pumping and regeneration) and foreseeable accidents with the cryo-pump. This paper describes a thermal-structural coupled analysis of the present TCPH according to the allowable stress criteria of RCC-MR, in which the worst cases and outcomes of various load combinations are obtained. Meanwhile, optimization of the structure has been carried out to obtain positive analysis results and an adequate safety margin.

Keywords: ITER, TCPH, thermal-structural coupled analysis, RCC-MR

PACS: *52.55.Fa, 28.52.-s*

DOI: 10.1088/1009-0630/14/11/10

1 Introduction

The international thermonuclear experimental reactor (ITER) is a torus-shaped double-wall structured tokamak. At its lower level, there are 8 ports for the torus cryo-pumps (Fig. 1) attached to the TCPH which are positioned and welded directly to the cryostat wall once they are installed in the tokamak pit.

Generally, the TCPH has the following functions [1]:

a. supporting the torus cryo-pumps;

b. connecting the cryo-pumps to the torus vacuum in the VV;

c. providing cryo-pump regeneration with adequate volume;

d. providing tritium confinement and a primary vacuum boundary;

e. and providing RH docking compatibility for remote handling maintenance of the cryo-pump.

Owing to complicated operating conditions, the impact produced by both the temperature and pressure boundary should be taken into account in considering different operation states. As a result, a thermal-structural analysis of the TCPH is crucial in making its design feasible and acceptable.

2 Design of the TCPH

To provide tritium confinement and a primary vacuum, double metal seals have been utilized on the bolted connection between the torus cryo-pump and the TCPH. Meanwhile, the mating flange on the TCPH shall match the dimensions and tolerances consistent with the cryo-pump flange. The surface unevenness

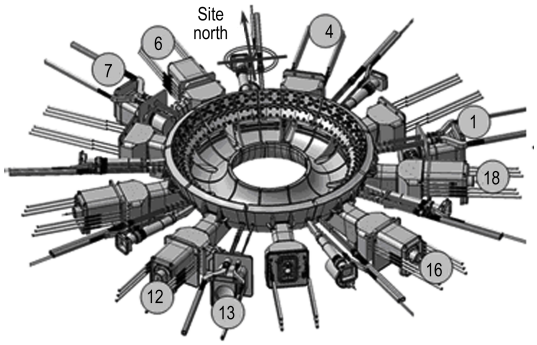

Fig.1 Eight locations for cryo-pump at lower ports

required in the seal region is assumed to be 0.8 μm, while perpendicularity to the axis should be less than 0.09 mm, by which the main vacuum seal will be better protected. The VV port extension and the TCPH are welded together by two co-axial cylindrical bellows to create the torus vacuum boundary. To achieve the purpose of separating the pump interior from the main vacuum, there is a valve on the cryo-pump which has two opposite cases during normal cryo-pump operation: one is when the valve is fully open; the other is when the valve is fully closed. When the valve is fully open the temperature of the pump is very low. The interior is connected to the VV to pump the gas mixture to achieve sufficient vacuum. When the valve is fully closed it is time for regeneration, with the temperature of the pump becoming high. Intermittent regeneration of the TCPH requires an isolated space from the main vacuum and warming of the pump interior. During this time the interior is open to the regeneration vacuum to regenerate the pump. The TCPH has been designed to maintain a regeneration volume of

*supported by International Thermonuclear Experimental Reactor (ITER) Specific Plan in China (2009GB101004)

6.5 m^3, which includes the attached piping and cryo-pump volume itself to achieve the purpose of keeping adequate volume. The remote handling flange is designed for indispensable remote handling procedures, which include removal of the regeneration pipes and the pump itself, and special pockets have been added to the TCPH, making it compatible with the above operations [2]. Fig. 2 illustrates the relative position of important components and the relationship among cryostat/TCPH/cryo-pump assembly.

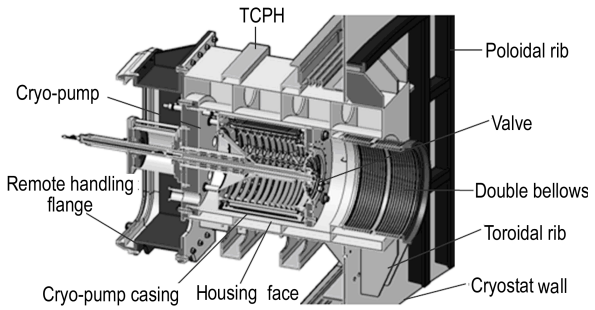

Fig.2 Cross section of a cryostat/TCPH/cryo-pump assembly

3 Finite element (FE) analysis of the TCPH

3.1 Description of the FE model

An isometric view of a 3D ANSYS FE model is shown in Fig. 3. The geometric model includes the TCPH, 1/18 segment of the cryostat with poloidal and toroidal reinforce ribs, the front flange for remote handling, and the simplified cryo-pump model. In thermal analysis, the FE model includes 620819 nodes and 137416 elements, in which CONTA174 and TARGE170 elements have been used to establish the contact between the TCPH and the cryo-pump to better simulate thermal conductivity, and the others consist of solid 90 and solid 87 elements. Accordingly, the elements are switched to solid 186 and solid 187 in structural analysis, while MASS21 is added to simulate the dead weight of the pump [3,4].

3.2 Materials and standard

TPCH has to be manufactured in 304L stainless steel in accordance with its design requirements, considering the possible temperature distribution appropriately. Various material properties depending on temperature are listed in Table 1 [5]. In this paper, RCC-MR is taken as the criterion for assessing the reliability of the TCPH. RCC-MR is the design and construction standard for mechanical components, applicable to the ITER Safety Important Component (SIC) in the design and manufacture phase. The ITER loading conditions are categorized into four classes from I to IV depending on their probability of occurring, which correspond to levels A, C and D in RCC-MR [6].

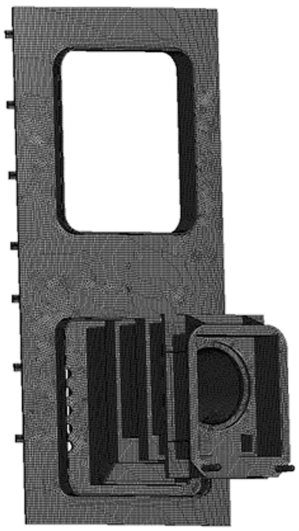

Fig.3 FE model of a cryostat/TCPH assembly

3.3 Boundary conditions (BC)

As 1/18th is modelled for the FE analysis, symmetric BC is applied to both sides of the cryostat; symmetric BC implies that in-plane rotations and out-of-plane translations are zero. The bottom of the cryostat is set as a fixed support to constrain all the degrees of freedom (DOF) to prevent any unconstrained movement.

3.4 Load condition [7,8]

3.4.1 Thermal analysis loads

Heat transmission between the TCPH and cryo-pump has to be confirmed by thermal analysis considering the following thermal loads:

a. Uniform temperature of cryostat/TCPH/cryo-pump assembly is kept at 25°C.

Table 1. Material properties of 304L stainless steel

Temperature (°C)	Density (kg/m^3)	Young's modulus (GPa)	Poisson's ratio	Mean thermal expansion ($\times 10^{-6}$, 1/°C)	Thermal conductivity (W/m°C)
20	7930	200	0.3	15.3	14.28
50	7919	197	0.3	15.5	14.73
100	7899	193	0.3	15.5	15.48
150	7879	189	0.3	16.2	16.23

b. The variation of temperature on the cryo-pump casing is between 93°C (T_a) in pumping operation and 127°C (T_b) in "water-like" 470 K regeneration mode.

c. 5 MW/m^{2}K is taken as a convection factor between the TCPH and its environment, which is a conservative estimate when there is no apparent wind flowing.

d. Radiation between the casing and housing face is considered to be surface to surface radiation, and the emissivity of both surfaces is assumed to be 0.4.

e. The thermal load generated by neutron radiation is negligible, considering the long distance and multiple shielding between the VV and TCPH.

3.4.2 Structural analysis loads

a. Thermal load

The temperature distribution obtained in the thermal analysis is taken as the inputs to carry out the subsequent structural analysis.

b. Gravitational load (DW)

The gravitational load due to the weight of the TCPH and cryostat with reinforced ribs is 45604 kg, while the weight of the cryo-pump is 8000 kg.

c. Pressure load

There are 4 kinds of pressure to be considered: internal to the cryostat (P_{in}), external to the cryostat and the TCPH (P_{ex}), the pressure between the casing and housing (P_{gap}), and the pressure in the cavity of the TCPH (P_{ca}). As shown in Table 2, all the complex pressure conditions have been considered and corresponding categories have been identified after comparison.

d. Maintenance force (F)

The maintenance force when the cryo-pump plug transfer cask operates should be considered, which is about 200 kN along the radial direction.

e. Electromagnetic load

Either during a plasma vertical displacement event (VDE) or a plasma major disruption (MD), the electromagnetic load is so small that it can be neglected.

f. Seismic load (SL)

Seismic load (SL) will be obtained after the modal analysis as shown in Table 3, where SL-1 corresponds to an event with a probability in the order of 10^{-2} per year, while all the safety related structures, systems, and components are functional after an SL-1 event without special maintenance; SL-2 corresponds to an event with a probability in the order of $10^{-4} \sim 10^{-6}$ per year, while gross damage to the affected systems or components has been made; nevertheless, the facility maintains the specified minimum safety function.

Table 3. Seismic acceleration affecting the TCPH model

	Seismic acceleration (m/s^2)		
	Radial	Toroidal	Vertical
SL-1	1.42	1.35	5.73
SL-2	4.25	4.06	17.2

3.5 Analysis result

3.5.1 Modal analysis

The modal analysis of the cryostat/TCPH/cryo-pump assembly has been carried out to estimate the natural frequencies and the mode shapes of the structure. The first and second natural frequencies of the structure are low at 11 Hz and 20 Hz, respectively, and its first mode shape including the natural frequency is shown in Fig. 4. Therefore, based on the result of the modal analysis, the corresponding seismic load is acquired as a consequence of the floor response spectrum, calculated with the influence of the soil-structure interaction and the influence of the building [9~11].

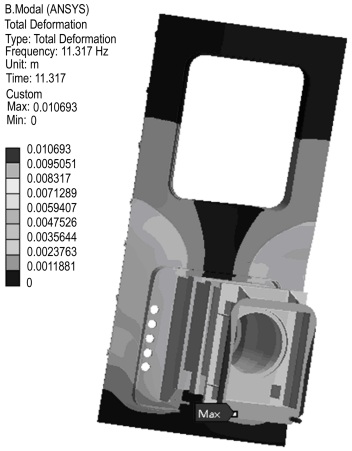

Fig.4 First mode shape for a cryostat/TCPH assembly

Table 2. Pressure load combinations

Category	P_{in}(MPa)	P_{ex}(MPa)	P_{gap}(MPa)	P_{ca}(MPa)	Events
P_I&P_{II}	0	0.1	0	0.002	Normal operation
	0.14	0.1	0	0.002	Air or helium ingress inside cryostat
P_{III}	0	0.1	0	0.15	Safety design requirement
	0.14	0.1	0	0.15	Safety design requirement
	0	0.1	0.15	0.002	Coolant leakage inside VV
P_{IV}	0.2	0.1	0	0.2	Cooling water and helium inside cryostant
	0	0.12	0	0.2	Coolant leakage outside cryostat
	0	0.1	0	0.2	Safety design requirement
	0.2	0.1	0	0.1	Regeneration pipes broken
	0.14	0.1	0	0.1	Regeneration pipes broken
	0	0.1	0.1	0	"water-like" 470 K regeneration mode

3.5.2 Thermal analysis

Steady-state thermal analysis of the cryostat/TCPH/ cryo-pump assembly using the finite element method has been performed aiming to acquire the temperature distribution and thermal gradient on the structure. The minimum temperature of the TCPH is −13 °C during the cryo-pump's pumping stage (Fig. 5(a)), while the maximum temperature of the TCPH is 99°C during the cryo-pump's regeneration stage (Fig. 5(b)). The thermal gradient at the corner approximate to the flange is much larger [12,13].

3.5.3 Thermal-structural coupled analysis

FE modeling results of the TCPH under complex load combinations have been obtained. It can be seen that the maximum stress intensity under all load categories is within the corresponding allowable stress defined in RCC-MR, whether the thermal condition is considered or not. The maximum displacement due to deformation is only 3.5 mm (Fig. 6(a)), which can be ignored when it is compared with the global dimension. The maximum stress intensity is 274 MPa under category II, which occurs at the internal rib of the TCPH (Fig. 7(a)), but there is a 23.8% margin to ensure safety. However, when there is no thermal load, the maximum stress intensity is 171 MPa, which occurs at the bottom of the poloidal reinforced rib of the cryostat (Fig. 6(b)), and the safety margin is only 5%; therefore, an optimization of the model is needed to obtain an adequate safety margin [14,15]. Two poloidal reinforced ribs in the proximity of the dangerous area have been added to resist the external force.

Using the same methodology, new results are obtained to reevaluate the stress intensity distribution. Both results, before and after optimization, are summarized in Table 4. The new results show that the maximum stress intensity is 307 MPa, which still occurs at the internal rib of the TCPH (Fig. 7(b)), but at different locations. The maximum stress intensity at the location of concern is 138 MPa, which is abundant under the allowable stress. As predicted, the margin of concern is 23.3%, which is apparently better than the previous model. At the same time, safety margins under some other categories have been reduced, all of them are not less than 14.7%, which is a desirable outcome.

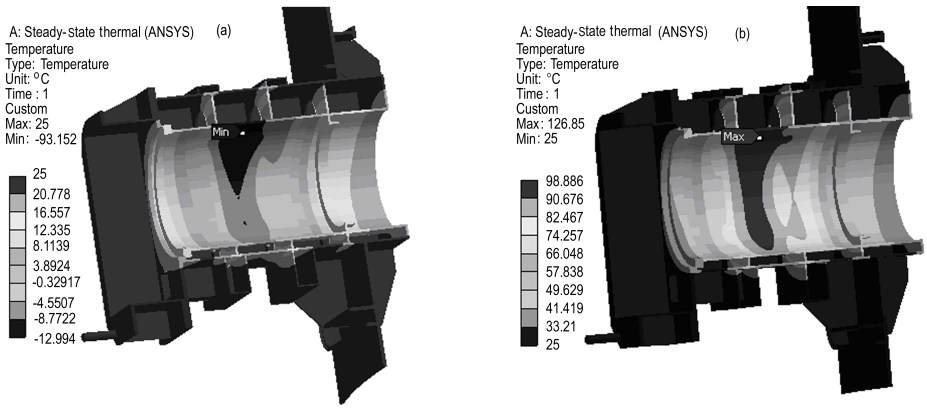

Fig.5 Temperature distribution, (a) Low temperature, (b) High temperature

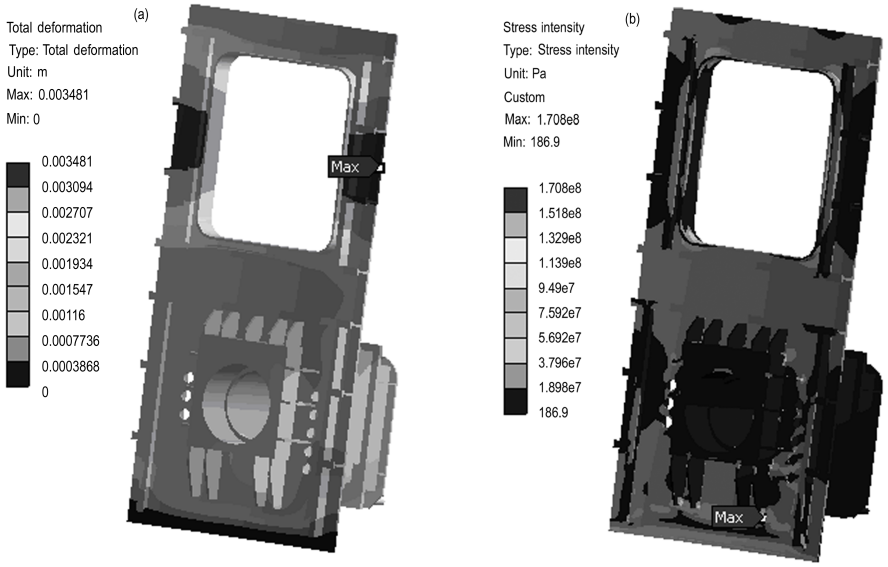

Fig.6 Displacement (a) and stress intensity (b) contour under the worst conditions

Table 4. Results summary of maximum stress intensity

Category	Load combination	Stress category	Allowable (MPa)	Stress intensity^{A} (MPa)	Margin /100	Stress intensity^{B} (MPa)	Margin /100
Category I&II	D+P_{II}	P_b+P_L	$1.5S_m^{I,II}$=180	113	37.2	115	36.1
	D+P_{II}+SL-1			146	18.8	126	30
	D+P_{II}+F			139	22.7	125	30.6
	D+P_{II}+F+SL-1			171	5	138	23.3
	D+P_{II}+T_a	$P_b + P_L + Q$	$3S_m^{I,II}$=360	141	60.8	142	60.6
	D+P_{II}+T_a+SL-1			154	57.2	143	60.3
	D+P_{II}+T_a+F			147	59.1	142	60.6
	D+P_{II}+T_a+F+SL-1			178	50.5	143	60.3
	D+P_{II}+T_b			273	24.1	301	16.4
	D+P_{II}+T_b+SL-1			274	23.8	305	15.3
	D+P_{II}+T_b+F			273	24.1	304	15.6
	D+P_{II}+T_b+F+SL-1			274	23.8	307	14.7
Category III	D+P_{III}	P_b+P_L	$1.5S_m^{III}$=243	123	49.3	117	51.9
	D+P_{III}+SL-1			156	35.8	129	46.9
Category IV	D+P_{IV}	P_b+P_L	$1.5S_m^{IV}$=432	132	69.4	118	72.7
	D+P_{IV}+SL-2			251	41.8	175	59.5

P_L is primary local membrane stress, P_b is primary bending stress, Q is secondary membrane plus bending stress, S_m is the allowable stress. ^{A} represents the results before optimization, ^{B} represents the results after optimization

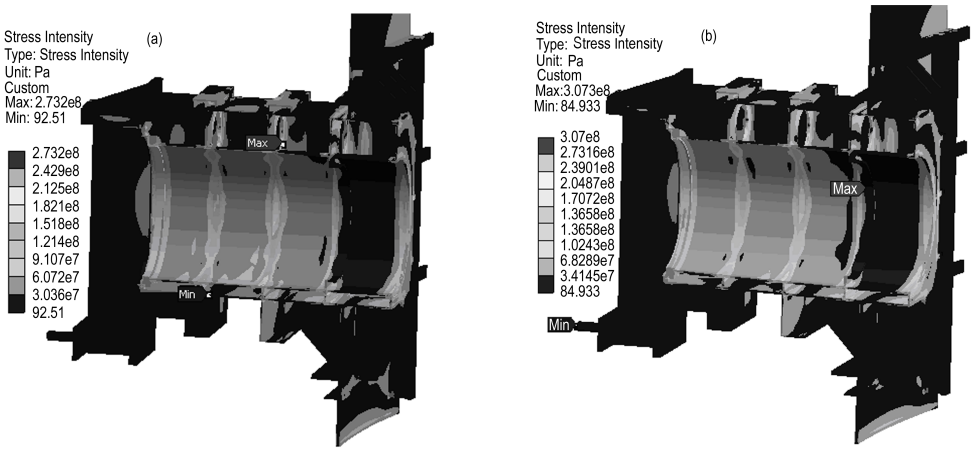

Fig.7 The maximum stress intensity (a) before optimization and (b) after optimization

4 Conclusion

As ITER SIC, the TCPH shall withstand different operating loads as well as complicated loads due to accidental events. To satisfy engineering requirements, steady-state thermal analysis has been performed by means of ANSYS software. The temperature distribution has been obtained. The elastic structural analysis has also been carried out to evaluate the displacement and stress intensity distribution. The results in all possible load combinations have been summarized; according to the allowable stress criteria of RCC-MR, the maximum stress intensities are all under the allowable stress, and a safety margin of at least 14.7% is obtained after modification.

Acknowledgements

The authors would like to express their sincere appreciation to Dr. B. DOSHI, J-M. MARTINEZ, and M. MEEKINS of the ITER organization for their help and stimulation during the study. The views and opinions expressed herein do not necessarily reflect those of the ITER Commission.

References

1 Bharat Doshi, Antipenkov Alexander, Bruno Levesy. 2010, Draft Preliminary Technical Input for Torus Cryo-Pump Housing and Associated Bellows. ITER-D-35TFJ5, France

2 A. Mack, A. Antipenkov, J.C. Boissin, et al. 2002, Fusion Engineering and Design, 61∼62: 611
3 Prosenjit Santra, Vijay Bedakihale, Tata Ranganath. 2009, Fusion Engineering and Design, 84: 1708
4 Cai Yingxiang, Yu Jie, Wu Songtao. 2007, Plasma Science and Technology, 9: 216
5 Barabash V. 2008, Summary of material data for structural analysis of the ITER vacuum vessel and ports. ITER-D-229D7N, France
6 French Society for Design and Construction Rules for Nuclear Island Components. 2007, RCC-MR, "Design and Construction Rules for Mechanical Components of FBR. Nuclear Island". AFCEN, Paris
7 Bachmann C. 2010, Load Specification for the ITER Vacuum Vessel. ITER-D-2F52JY, France
8 Zhou C, Doshi B. 2010, Load Specification for the ITER Cryostat. ITER-D-34HHUG, France
9 Sannazzaro G, Mazzone G. 2010, Template for analysis document on calculation of ITER tokamak complex seismic loads from heavy equipment. ITER-D-3V74UZ, France
10 Sorin V. 2011, Seismic analyses of the tokamak building complex and the main tokamak components. ITER-D-3ZS67G, France
11 Sorin V, Mazzone G. 2010, Seismic Analysis of the Tokamak Building. ITER-D-3USBZ4, France
12 Song Yuntao, Yao Damao, Du Shijun, et al. 2006, Plasma Science and Technology, 8: 221
13 L. Petrizzi, M. Loughlin, A. Martin, et al. 2009, Fusion Engineering and Design, 84: 1505
14 Xie Han, Song Yuntao, Yao Damao, et al. 2010, Plasma Science and Technology, 12: 738
15 J-M. Martinez. 2010, Analysis of the Structural Margin of the Reinforced VV Lower Port Poloidal Gussets. ITER-D-2LNFJN, France

(Manuscript received 30 May 2011)
(Manuscript accepted 17 October 2011)
E-mail address of WANG Songke: wsongk@ipp.ac.cn